

3

General Features of Experimental Methods

3.1 The electromagnetic spectrum

In a vacuum all electromagnetic radiation travels at the same speed, the speed of light c , and may be characterized by its wavelength λ , in air or vacuum, or by its wavenumber $\tilde{\nu}$ or frequency ν , both conventionally in a vacuum, where

$$\lambda_{\text{vac}} = \frac{c}{\nu} = \frac{1}{\tilde{\nu}} \quad (3.1)$$

Figure 3.1 illustrates the extent of the electromagnetic spectrum from low-energy radiowave to high-energy γ -ray radiation. The division into the various named regions does not imply any fundamental differences but is useful to indicate that different experimental techniques are used. Indications of region boundaries, which should not be regarded as clear cut, are given in wavelength (mm, μm or nm), frequency (GHz) and wavenumber (cm^{-1}). In addition, in the high-energy regions the energy is indicated in electron volts (eV) where

$$1 \text{ eV} = hc(8065.54 \text{ cm}^{-1}) = h(2.417 99 \times 10^{14} \text{ s}^{-1}) \quad (3.2)$$

Also indicated in Figure 3.1 are the processes that may occur in an atom or molecule exposed to the radiation. A molecule may undergo rotational, vibrational, electronic or ionization processes, in order of increasing energy (typical ranges are indicated). A molecule may also scatter light in a Raman process, and the light source for such an experiment is usually in the visible or near-ultraviolet region (see, however, Section 5.3.1). An atom may undergo only an electronic transition or ionization since it has no rotational or vibrational degrees of freedom. Nuclear magnetic resonance (NMR) and electron spin resonance (ESR) processes involve transitions between nuclear spin and electron spin states, respectively, but these spectroscopies necessitate the sample being between the poles of a magnet and will not be covered in this book.

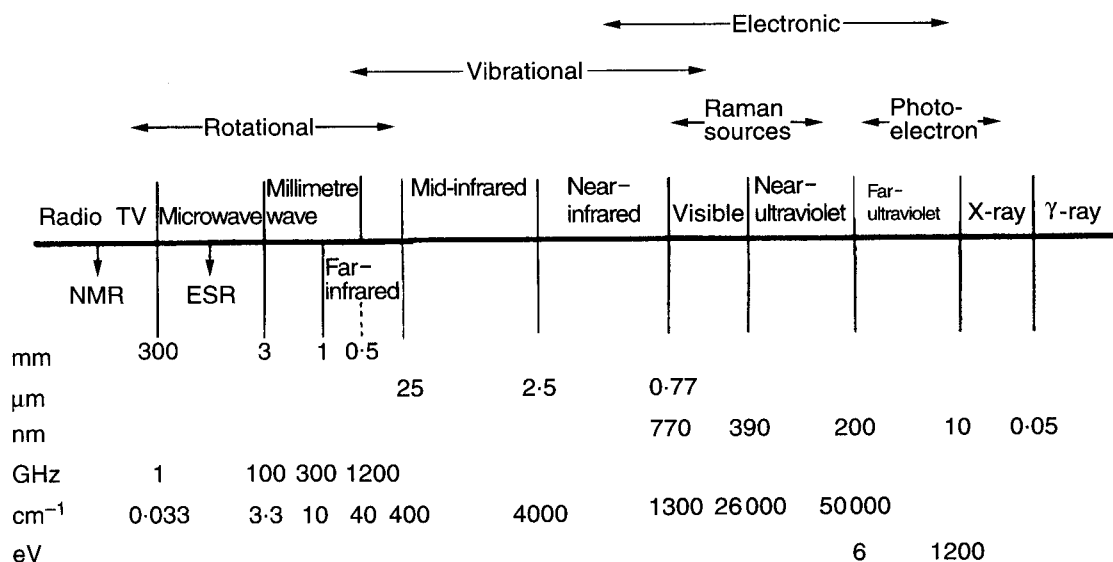


Figure 3.1 Regions of the electromagnetic spectrum

3.2 General components of an absorption experiment

Emission spectroscopy is confined largely to the visible and ultraviolet regions, where spectra may be produced in an arc or discharge or by laser excitation. Absorption spectroscopy is, generally speaking, a more frequently used technique in all regions of the spectrum and it is for this reason that we shall concentrate rather more on absorption.

Figure 3.2 shows schematically the four main components – source, cell, dispersing element and detector – of an absorption experiment. The source is ideally a continuum in which radiation is emitted over a wide wavelength range with uniform intensity. The absorption cell containing the sample must have windows made from a material which transmits the radiation and it must also be long enough for the absorbance (Equation 2.16) to be sufficiently high.

The choice of phase of the sample is important. Generally, in high-resolution spectroscopy (see Section 3.3.1 for a discussion of resolution), the sample is in the gas phase at a pressure which is sufficiently low to avoid pressure broadening (see Section 2.3.3). In the liquid

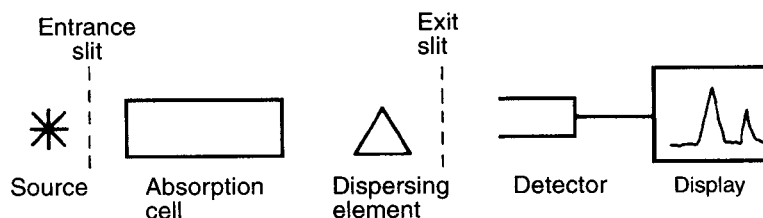


Figure 3.2 The components of a typical absorption experiment

phase all rotational structure is lost and vibrational structure is considerably broadened but is important in, for example, the use of infrared spectroscopy as an analytical tool or obtaining oscillator strengths (see Equation 2.18) by measuring the area under an electronic absorption curve. In the solid phase, in which the sample may be a pure crystal, mixed crystal or solid solution in, say, a frozen noble gas, rotational motion is quenched as the molecules are held rigidly. Vibrational and electronic transitions are generally broad at normal temperatures but may be dramatically sharpened at liquid helium temperature (*ca* 4 K).

The dispersing element to be described in Section 3.3 splits up the radiation into its component wavelengths and is likely to be a prism, diffraction grating or interferometer, but microwave and millimetre wave spectroscopy do not require such an element.

The detector must be sensitive to the radiation falling on it, and the spectrum is very often displayed on a chart recorder. The spectrum may be a plot of absorbance or percentage transmittance ($100I/I_0$; see Equation 2.16) as a function of frequency or wavenumber displayed linearly along the chart paper. Wavelength is not normally used because, unlike frequency and wavenumber, it is not proportional to energy. Wavelength relates to the optics rather than the spectroscopy of the experiment.

3.3 Dispersing elements

3.3.1 Prisms

Although prisms, as dispersing elements, have been largely superseded by diffraction gratings and interferometers they still have uses in spectroscopy and they also illustrate some important general points regarding dispersion and resolution.

Figure 3.3 shows a prism of base length b with one face filled with radiation from a white light source made parallel by lens L_1 . The prism disperses and resolves the radiation, which is focused by L_2 onto a detector. If wavelengths λ and $\lambda + d\lambda$ are just observably separated then $d\lambda$, or the corresponding frequency interval dv or wavenumber interval $d\tilde{\nu}$, is the resolution which is obtained.¹ The resolving power R of a dispersing element is defined as

$$R = \frac{\lambda}{d\lambda} = \frac{\nu}{d\nu} = \frac{\tilde{\nu}}{d\tilde{\nu}} \quad (3.3)$$

and, for a prism,

$$R = b \frac{dn}{d\lambda} \quad (3.4)$$

provided that the face of the prism is filled by the incident beam. In Equation (3.4) n is the refractive index of the prism material and, for high resolving power, $dn/d\lambda$ should be large. This happens as we approach a wavelength at which the material absorbs radiation. For

¹ We refer to an observation as 'high resolution' or 'low resolution' when $d\lambda$, dv or $d\tilde{\nu}$ is small or large, respectively.

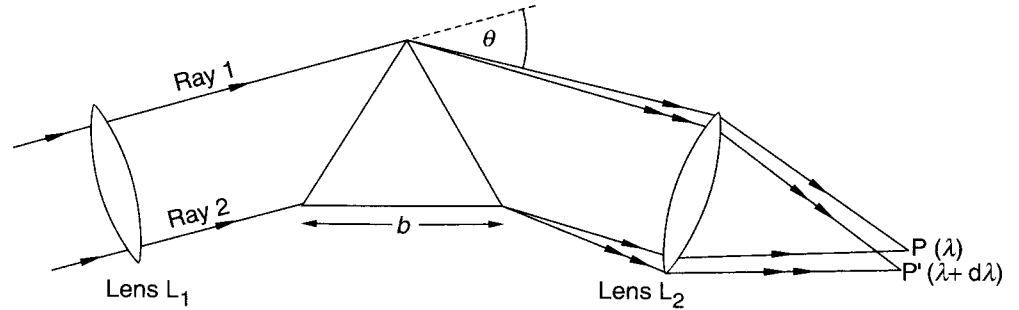


Figure 3.3 Dispersion by a prism

glass, absorption occurs at $\lambda < ca$ 360 nm and, therefore, the resolving power is greatest in the blue and violet regions, whereas quartz absorbs at $\lambda < ca$ 185 nm and its resolving power is greatest in the 300 nm to 200 nm region and rather low in the visible region.

If, in Figure 3.3, P and P' are a distance $d\ell$ apart then the linear dispersion is defined as $d\ell/d\lambda$ whereas the angular dispersion is defined as $d\theta/d\lambda$, where θ is the angle shown.

We have said that wavelengths λ and $\lambda + d\lambda$ are just observably separated, or resolved, but we have not established a criterion for judging that this is so. It was Rayleigh who proposed such a criterion, illustrated in Figure 3.4. If we imagine a narrow entrance slit before lens L_1 in Figure 3.3 the detector sees not just an image of the slit at wavelength λ but a diffraction pattern as shown in Figure 3.4(a) with intensity minima at $\pm\lambda$, $\pm 2\lambda$, ... from the central maximum. Rayleigh suggested that if the two diffraction patterns corresponding to points P and P' in Figure 3.3 are such that the central maximum of P' is no closer to that of P than is the first minimum of P, as in Figure 3.4(b), then P and P' are said to be just resolved.

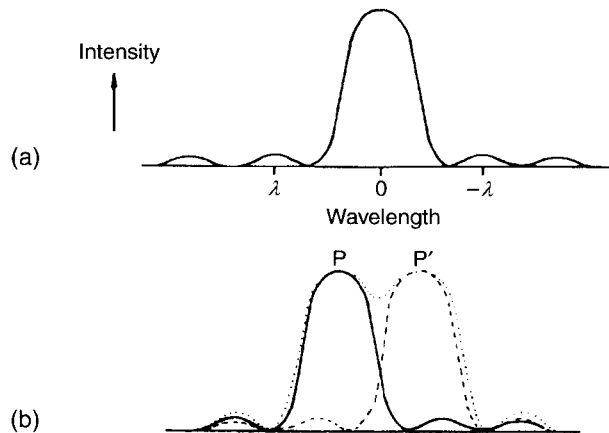


Figure 3.4 (a) Diffraction pattern produced by a narrow slit. (b) The Rayleigh criterion for resolution

It is important to realize that a line in a spectrum is an image of the entrance slit formed at a particular wavelength, the image being a diffraction pattern like that in Figure 3.4(a). Therefore, as the slit is widened the main peak in the diffraction pattern is widened and the resolution of which the dispersing element is capable is effectively reduced. However, when the slit width is reduced there comes a point when the observed line width is not reduced any further even though the dispersing element may be capable of extremely high resolution. This point is likely to occur when the line width is limited by pressure or Doppler broadening (see Sections 2.3.2 and 2.3.3).

3.3.2 Diffraction gratings

A diffraction grating consists of a series of parallel grooves ruled on a hard glassy or metallic material. The grooves are extremely closely spaced, a spacing of the order of $1\ \mu\text{m}$ being not unusual. Gratings are usually coated on the ruled surface with a reflecting material such as aluminium so that the grating acts also as a mirror. The surface may be plane or concave, the latter type serving to focus as well as disperse and reflect the light falling on it.

Figure 3.5 shows how white light falling at 90° to the surface of a reflection grating G is dispersed. The general equation for diffraction by a grating is

$$m\lambda = d(\sin i + \sin \theta) \quad (3.5)$$

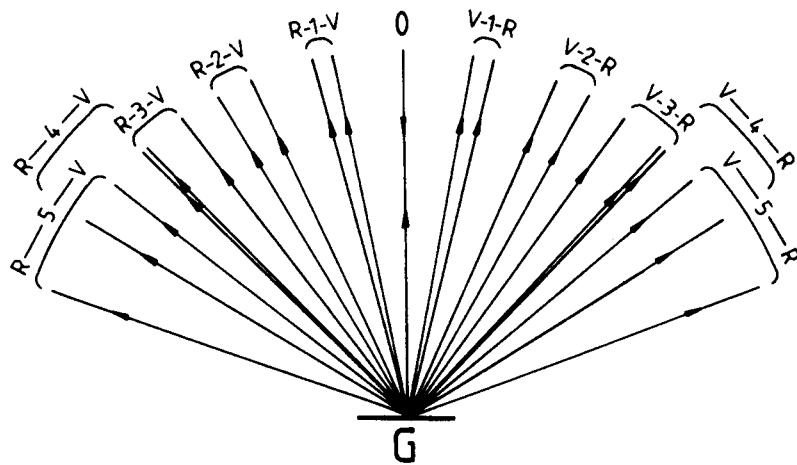


Figure 3.5 Various orders of diffraction from a plane reflection grating G; R indicates the red end of the spectrum; V indicates the violet end of the spectrum; the central number is the order of diffraction

where i and θ are the angles of incidence and reflection, respectively, both measured from the normal to the surface, d is the groove spacing, λ the wavelength, and m ($= 0, 1, 2, \dots$) the order of diffraction. For normal incidence

$$m\lambda = d \sin \theta \quad (3.6)$$

The angular dispersion produced by the grating is given by

$$\frac{d\theta}{d\lambda} = \frac{m}{d \cos \theta} \quad (3.7)$$

and the figure shows how it increases with the order, the dispersion shown being from violet (V) to red (R) in each order. The resolving power R (Equation 3.3) of a grating is given by

$$R = mN \quad (3.8)$$

where N is the total number of grooves, but, of course, all the grooves must receive the incident light if the resolving power is to be fully realized. When we require high dispersion and high resolution from a grating it is clear, from Equations (3.7) and (3.8), that we should use as high an order as possible. Figure 3.5 shows that in higher orders there is an increasing problem of overlapping with adjacent orders. This may be avoided by filtering or pre-dispersion, with a small prism or grating, of the incident light.

If we are using only one order of diffraction it is very wasteful to reject the radiation diffracted in other orders and also that in the same order but on the other side of the incident beam. The radiation can be diffracted preferentially close to a particular angle by using a blazed grating. Grating grooves are ruled by a diamond and would normally be symmetrically V-shaped but, if they are ruled so that each has a long and a short side, as in Figure 3.6, reflection will be most efficient when the incident and diffracted beams make an angle ϕ to the normal N to the grating surface as shown: the beams are normal to the long

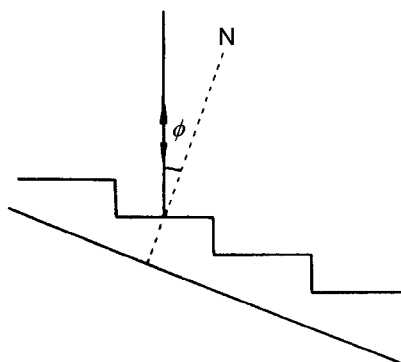


Figure 3.6 Use of a blazed grating at the blaze angle ϕ ; N is the normal to the grating surface

side of the groove. The angle ϕ is called the blaze angle, and when the grating is used with equal angles of incidence and reflection, as in the figure, Equation (3.5) becomes

$$m\lambda = 2d \sin \theta \quad (3.9)$$

Diffraction gratings may be made by a holographic process, but blaze characteristics cannot be controlled and their efficiency is low in the infrared. They are mostly used for low-order work in the visible and near-ultraviolet.

Worked example 3.1

Question. A diffraction grating has a ruled area that is 10.40 cm wide, has 600.0 grooves per millimetre and is blazed at an angle of 45.00° .

- What is the wavelength of radiation diffracted at the blaze angle in the first, fourth and ninth orders?
- What is the resolving power in these orders?
- What is the resolution in terms of wavelength (nm), wavenumber (cm^{-1}) and frequency (GHz) in the ninth order at 300 nm?

Answer:

- The grating is 104.0 mm wide. Thus the total number of grooves is given by

$$N = 104.0 \text{ mm} \times 600.0 \text{ mm}^{-1} = 62\,400$$

and the spacing between grooves by

$$\begin{aligned} d &= \frac{0.1040 \text{ m}}{62\,400} \\ &= 1.6667 \times 10^{-6} \text{ m} \\ &= 1666.7 \text{ nm} \end{aligned}$$

The Bragg equation for diffraction is given by Equation (3.9):

$$\begin{aligned} m\lambda &= 2d \sin \theta \\ &= 2 \times 1666.7 \text{ nm} \times 0.70711 \\ &= 2357.1 \text{ nm} \\ \therefore \lambda &= \begin{cases} 2357 \text{ nm} & \text{for } m = 1 \\ 589.3 \text{ nm} & \text{for } m = 4 \\ 261.9 \text{ nm} & \text{for } m = 9 \end{cases} \end{aligned}$$

(b) The resolving power R of the grating is given by Equation (3.8) as

$$\begin{aligned}
 R &= mN \\
 &= 62\,400m \\
 \therefore R &= \begin{cases} 62\,400 & \text{for } m = 1 \\ 249\,600 & \text{for } m = 4 \\ 561\,600 & \text{for } m = 9 \end{cases}
 \end{aligned}$$

(c) The resolution $d\lambda$, $d\tilde{\nu}$ or dv is obtained from the resolving power by using Equation (3.3)

$$\begin{aligned}
 R &= \frac{\lambda}{d\lambda} = \frac{\tilde{\nu}}{d\tilde{\nu}} = \frac{v}{dv} \\
 \therefore d\lambda &= \frac{\lambda}{R} = \frac{300.0 \text{ nm}}{561\,600} \\
 &= 5.342 \times 10^{-4} \text{ nm}
 \end{aligned}$$

For $\lambda = 300.0 \text{ nm}$,

$$\begin{aligned}
 \tilde{\nu} &= \frac{1}{\lambda} = \frac{1}{300.0 \text{ nm}} = \frac{1}{300.0 \times 10^{-7} \text{ cm}} = 33\,333 \text{ cm}^{-1} \\
 \therefore d\tilde{\nu} &= \frac{\tilde{\nu}}{R} = \frac{33\,333 \text{ cm}^{-1}}{561\,600} \\
 &= 0.05935 \text{ cm}^{-1}
 \end{aligned}$$

For $\lambda = 300.0 \text{ nm}$,

$$\begin{aligned}
 v &= \frac{c}{\lambda} = \frac{2.998 \times 10^{10} \text{ cm s}^{-1}}{300.0 \times 10^{-7} \text{ cm}} = 9.9933 \times 10^{14} \text{ s}^{-1} \\
 &= 9.9933 \times 10^5 \text{ GHz} \\
 \therefore dv &= \frac{v}{R} = \frac{9.9933 \times 10^5 \text{ GHz}}{561\,600} \\
 &= 1.779 \text{ GHz}
 \end{aligned}$$

3.3.3 Fourier transformation and interferometers

A thin layer of oil on water often shows regions of different colours, and this illustrates a third method of dispersing light. White light falling on the oil is reflected backwards and forwards within the layer, a part of the beam emerging from the surface each time. The various emerging beams may interfere constructively or destructively with each other, depending on the wavelength, and give rise to the different colours observed. This principle is made use of in an interferometer, which is used to disperse infrared, visible or ultraviolet radiation but is especially important for infrared radiation.

We shall discuss infrared interferometers in Section 3.3.3.2 but, before this, we need to understand the principles of Fourier transformation since this is involved in the very important step in treating the signal from an interferometer. This signal does not resemble the kind of spectrum that we usually obtain from a spectrometer and it is the modification of the signal to the intensity-versus-wavelength type of spectrum which we require that involves Fourier transformation. The principles of Fourier transformation are probably easier to understand when applied to longer wavelength radiofrequency radiation than to shorter wavelength infrared, visible or ultraviolet radiation. We shall consider radiofrequency radiation first.

3.3.3.1 Radiofrequency radiation

Consider radiofrequency radiation with a frequency of 100 MHz, or a wavelength of 3 m. Such radiation is used, for example, in a nuclear magnetic resonance (NMR) spectrometer and as a carrier of FM (or VHF) radio signals. Frequencies typical of radiofrequency radiation are relatively low compared with, say, near-infrared radiation of frequency 10 000 GHz (see Figure 3.1). Consequently there is no problem in producing detectors that can respond sufficiently rapidly to determine the frequency of a radiofrequency signal directly. If we consider a source of monochromatic radiofrequency radiation, the detector responds to the electric field E which is oscillating, as in Figure 2.1, at a frequency ν . The variation of the signal detected, $f(t)$, with time t is shown in Figure 3.7(a) and is said to be the spectrum in the time domain. In this case it is the spectrum of a monochromatic source.

We are more used to spectra recorded not in the time domain but in the frequency (or wavenumber or wavelength) domain in which the detector signal is plotted against, say, frequency ν rather than time t . We can easily see that the time domain spectrum in Figure 3.7(a) corresponds to the frequency domain spectrum in Figure 3.7(b) in which the signal $F(\nu)$ is plotted against frequency. The monochromatic source produces a single line spectrum.

The process of going from the time domain spectrum $f(t)$ to the frequency domain spectrum $F(\nu)$ is known as Fourier transformation. In this case the frequency of the line, say 100 MHz, in Figure 3.7(b) is simply the value of ν which appears in the equation

$$f(t) = A \cos 2\pi\nu t \quad (3.10)$$

for the time domain spectrum, where A is the amplitude of $f(t)$.

If the source emits radiofrequency radiation consisting of two frequencies, ν and $\frac{1}{4}\nu$, of the same amplitude then

$$f(t) = A[\cos 2\pi\nu t + \cos 2\pi(\frac{1}{4}\nu)t] \quad (3.11)$$

and this is shown in Figure 3.8(a). The corresponding frequency domain spectrum is illustrated in Figure 3.8(b), which shows two equally intense lines, one at 100 MHz and the other at 25 MHz.

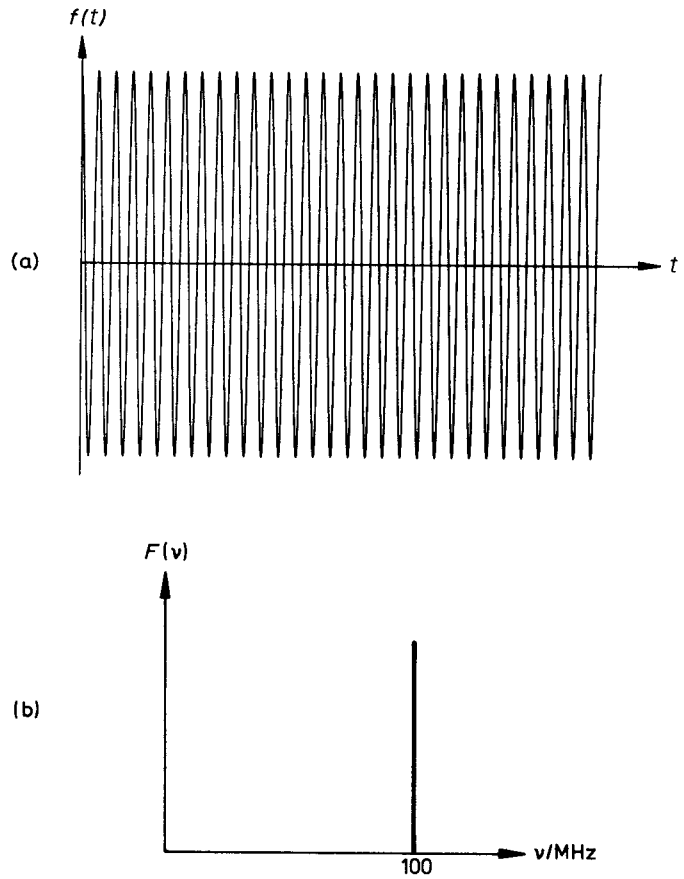


Figure 3.7 (a) The time domain spectrum and (b) the corresponding frequency domain spectrum for radiation of a single frequency

The sum of the two cosine waves in Figure 3.8(a) shows a beating between the waves. In general, if the two frequencies are ν_1 and ν_2 , the beat frequency, ν_B , is given by

$$\nu_B = |\nu_1 - \nu_2| \quad (3.12)$$

In the example in Figure 3.8, ν_B is 75 MHz.

Figure 3.9(a) shows a time domain spectrum corresponding to the frequency domain spectrum in Figure 3.9(b) in which there are two lines, at 25 and 100 MHz, with the latter having half the intensity of the former, so that

$$f(t) = \frac{1}{2}A \cos 2\pi\nu t + A \cos 2\pi\left(\frac{1}{4}\nu\right)t \quad (3.13)$$

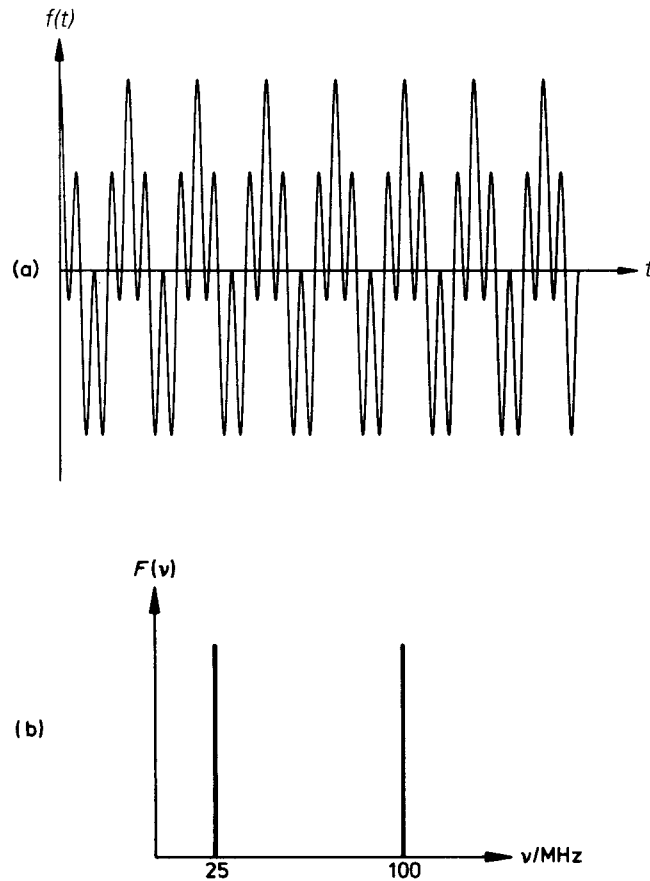


Figure 3.8 (a) The time domain spectrum and (b) the corresponding frequency domain spectrum for radiation of two different frequencies with a 1 : 1 intensity ratio

Conceptually, the problem of going from the time domain spectra in Figures 3.7(a)–3.9(a) to the frequency domain spectra in Figures 3.7(b)–3.9(b) is straightforward, at least in these cases because we knew the result before we started. Nevertheless, we can still visualize the breaking down of any time domain spectrum, however complex and irregular in appearance, into its component waves, each with its characteristic frequency and amplitude. Although we can visualize it, the process of Fourier transformation which actually carries it out is a mathematically complex operation. The mathematical principles will be discussed only briefly here.

In general, the time domain spectrum can be expressed as

$$f(t) = \int_{-\infty}^{+\infty} F(v) \exp(i2\pi vt) dv \quad (3.14)$$

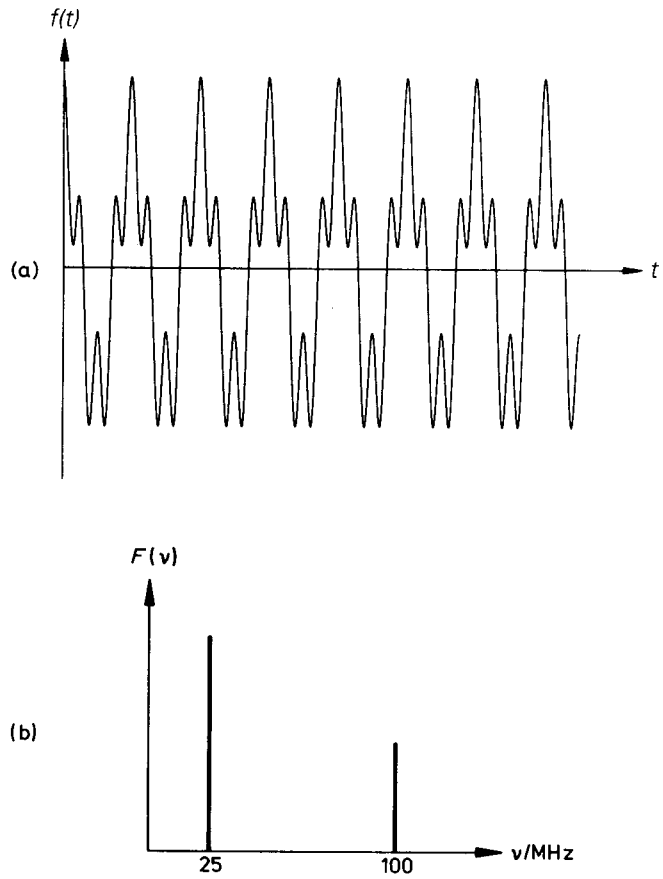


Figure 3.9 (a) The time domain spectrum and (b) the corresponding frequency domain spectrum for radiation of two different frequencies with a 2 : 1 intensity ratio

where $i = \sqrt{-1}$ and $F(v)$ is the frequency domain spectrum we require, but, because

$$\exp(i\phi t) = \cos \phi t + i \sin \phi t \quad (3.15)$$

Equation (3.14) becomes

$$f(t) = \int_{-\infty}^{+\infty} F(v)(\cos 2\pi vt + i \sin 2\pi vt)dv \quad (3.16)$$

For our purposes we can neglect the imaginary part of Equation (3.16), $i \sin 2\pi vt$, and then it is apparent that $f(t)$ is a sum of cosine waves, as we had originally supposed. Fourier transformation allows us to go from $f(t)$ to $F(v)$ by the relationship

$$F(v) = \int_{-\infty}^{+\infty} f(t) \exp(-i2\pi vt)dt \quad (3.17)$$

or, using the fact that

$$\exp(-i\phi t) = \cos \phi t - i \sin \phi t \quad (3.18)$$

we get

$$F(\nu) = \int_{-\infty}^{+\infty} f(t)(\cos 2\pi\nu t - i \sin 2\pi\nu t)dt \quad (3.19)$$

where, again, we can neglect the imaginary part, $i \sin 2\pi\nu t$.

A computer digitizes the time domain spectrum $f(t)$ and carries out the Fourier transformation to give a digitized $F(\nu)$. Then digital-to-analogue conversion gives the frequency domain spectrum $F(\nu)$ in the analogue form in which we require it.

In the case of a radio operating in the FM wavelength band, or indeed any wavelength band, the aerial receives a signal which contains all the transmitted frequencies. What the radio does is, effectively, to Fourier transform the signal so that we can tune in to any of the frequencies without interference from any others.

There is one important point, however, that we have neglected so far. Real spectra in the frequency domain do not look like those in Figures 3.7(b)–3.9(b): the lines in the spectra are not stick-like and infinitely sharp but have width and shape.

If the radiofrequency spectrum is due to emission of radiation between pairs of states – for example nuclear spin states in NMR spectroscopy – the width of a line is a consequence of the lifetime, τ , of the upper, emitting state. The lifetime and the energy spread, ΔE , of the upper state are related through the uncertainty principle (see Equation 1.16) by

$$\tau\Delta E \geq \hbar \quad (3.20)$$

or, since $\Delta E = h\Delta\nu$,

$$\Delta\nu \geq \frac{1}{2\pi\tau} \quad (3.21)$$

The effect of the lifetime of the upper state can be seen in the frequency domain spectrum by irradiating the sample with a short pulse of radiofrequency radiation and observing the decay of the signal. Figure 3.10(a) shows a similar time domain spectrum to that in Figure 3.8(a) but with a time decay superimposed on it. The Fourier transformed spectrum, in Figure 3.10(b), shows two lines having widths given by Equation (3.21).

The result in Equation (3.21) also shows that if $\tau = \infty$, as in the examples in Figures 3.7(a)–3.9(a), then $\Delta\nu = 0$ and the lines are infinitely sharp.

Fourier transform spectroscopy in the radiofrequency region has been applied most importantly in pulsed Fourier transform NMR spectroscopy, which is not a subject which

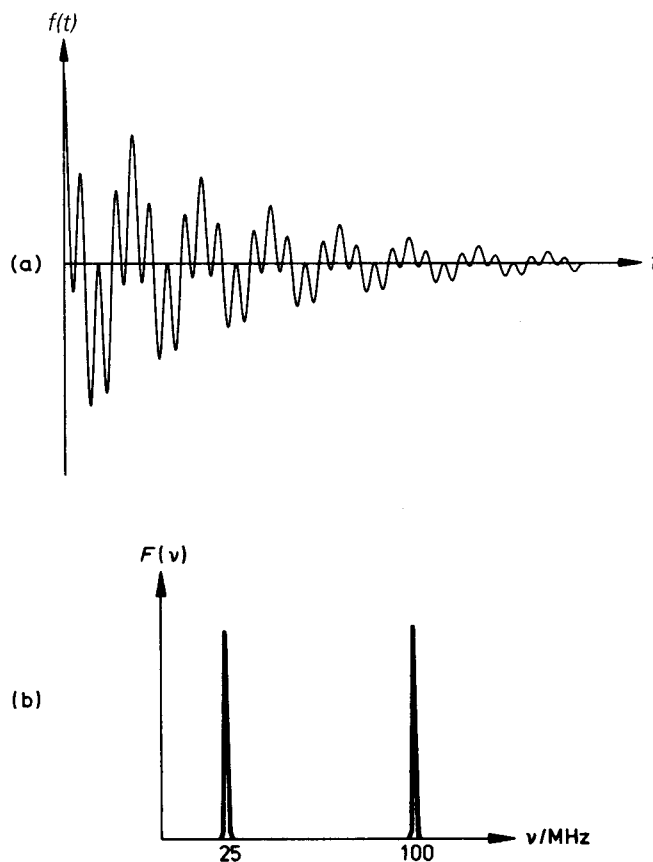


Figure 3.10 (a) Time domain and (b) frequency domain spectra corresponding to those in Figure 3.8 but in which the two lines are broadened

will be treated in detail here.² More recently, it has become a very important technique when applied to microwave spectroscopy.

There are now alternative ways for us to record an emission spectrum such as that in Figure 3.8. We can either record the time domain spectrum and Fourier transform to the frequency domain spectrum or obtain the frequency domain spectrum directly, in the more usual way, by scanning through the frequency range and recording the signal at the detector. However, there is an important advantage in recording the time domain spectrum: all the frequencies in the spectrum are recorded all the time. This is known as the multiplex or Fellgett advantage and results in a comparable spectrum being obtained in a much shorter time. Consequently, the Fourier transform (FT) technique can be used, for example, to obtain spectra of transient species formed during a chemical reaction.

² See, for example, Abraham, R. J., Fisher, J. and Loftus, P. (1988) *Introduction to NMR Spectroscopy*, Wiley, Chichester.

3.3.3.2 Infrared, visible and ultraviolet radiation

For radiofrequency and microwave radiation there are detectors which can respond sufficiently quickly to the low frequencies (<100 GHz) involved and record the time domain spectrum directly. For infrared, visible and ultraviolet radiation the frequencies involved are so high (>600 GHz) that this is no longer possible. Instead, an interferometer is used and the spectrum is recorded in the length domain rather than the frequency domain. Because the technique has been used mostly in the far-, mid- and near-infrared regions of the spectrum the instrument used is usually called a Fourier transform infrared (FTIR) spectrometer although it can be modified to operate in the visible and ultraviolet regions.

The most important component of an FTIR spectrometer is an interferometer based on the original design by Michelson in 1891, as shown in Figure 3.11.

For simplicity we consider a source S of monochromatic radiation entering the interferometer. A ray from this source strikes the beamsplitter B , which is coated on its second surface with a material that makes it half transmitting (ray 2) and half reflecting (ray 1). Ray 1 is then reflected by the movable mirror M_1 back through B to a detector D , while ray 2 is reflected by the fixed mirror M_2 and part is then reflected by B to the detector. C is a compensating plate introduced so that each of rays 1 and 2 has passed twice through the same length of the material from which both B and C are made. When they reach D , rays 1 and 2 have traversed different paths with a path difference δ . This is called the retardation and its magnitude depends on the position of M_1 . Figure 3.12(a) shows that, if $\delta = 0, \lambda, 2\lambda, \dots$, the two rays interfere constructively at the detector, whereas Figure 3.12(b) shows that, if $\delta = \lambda/2, 3\lambda/2, 5\lambda/2, \dots$, they interfere destructively and no signal is detected. Therefore, if δ is changed smoothly from zero the detected signal intensity $I(\delta)$ changes like a cosine function, as in Figure 3.13.

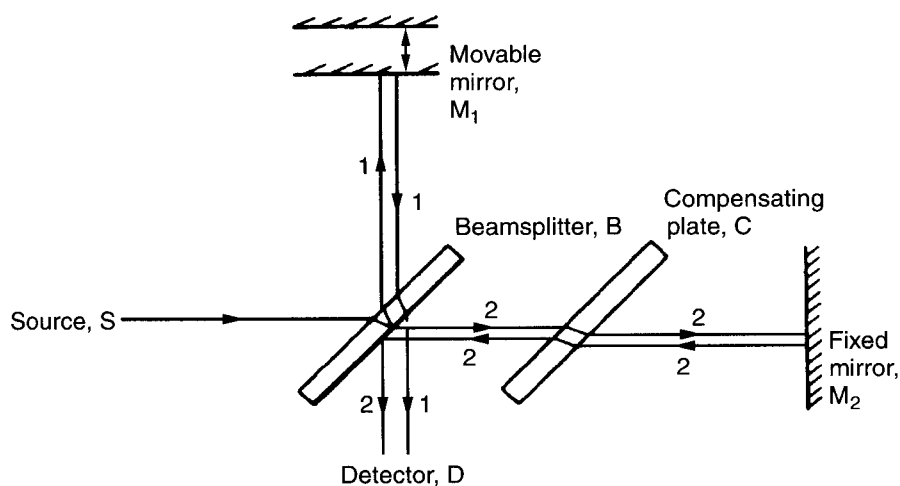


Figure 3.11 Michelson interferometer

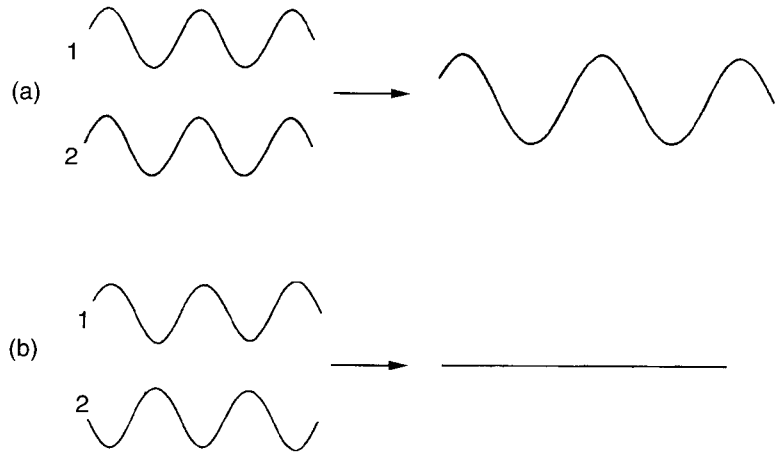


Figure 3.12 (a) Constructive and (b) destructive interference between rays 1 and 2 of monochromatic radiation

In a more usual emission experiment the source contains many wavelengths, the detector sees intensity due to many cosine waves of different wavelengths and the detected intensity is of the form

$$I(\delta) = \int_0^{\infty} B(\tilde{\nu}) \cos 2\pi\tilde{\nu}\delta \, d\tilde{\nu} \quad (3.22)$$

where $\tilde{\nu}$ is the wavenumber of the radiation and $B(\tilde{\nu})$ is the source intensity at that wavenumber (neglecting small corrections for variable beamsplitter efficiency and detector response). A plot of $B(\tilde{\nu})$ against $\tilde{\nu}$ is the dispersed spectrum of the source and is obtained by the procedure of Fourier transformation discussed in Section 3.3.3.1, giving

$$B(\tilde{\nu}) = 2 \int_0^{\infty} I(\delta) \cos 2\pi\tilde{\nu}\delta \, d\delta \quad (3.23)$$

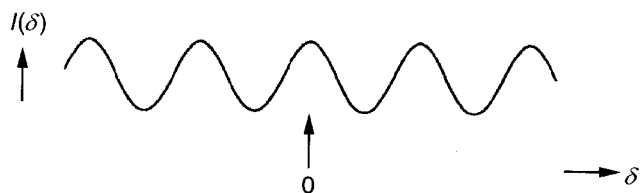


Figure 3.13 Change of signal intensity $I(\delta)$ with retardation δ

The majority of infrared spectra are obtained by an absorption rather than an emission process and, as a result, the change of signal intensity $I(\delta)$ with retardation δ appears very different from that in Figure 3.13.

Consider an infrared source emitting a wide range of wavenumbers for use in an absorption experiment. Figure 3.14(a) shows how the idealized wavenumber domain spectrum of this source, emitting continuously between $\tilde{\nu}_1$ and $\tilde{\nu}_2$, might appear. We can regard this spectrum as comprising a very large number of wavenumbers between $\tilde{\nu}_1$ and $\tilde{\nu}_2$ so that the corresponding detector signal, as a function of retardation, will be the result of adding together very many cosine waves of different wavelengths. The signal is large at $\delta = 0$ since all the waves are in phase, but elsewhere they are out of phase, interfere with each other and produce total cancellation of the signal. The intense signal at $\delta = 0$ is known as the centre burst and is shown in Figure 3.14(b). (Because of slight dispersion by the beamsplitter B the waves at $\delta = 0$ are not quite in phase, resulting in an asymmetry of the centre burst about $\delta = 0$.)

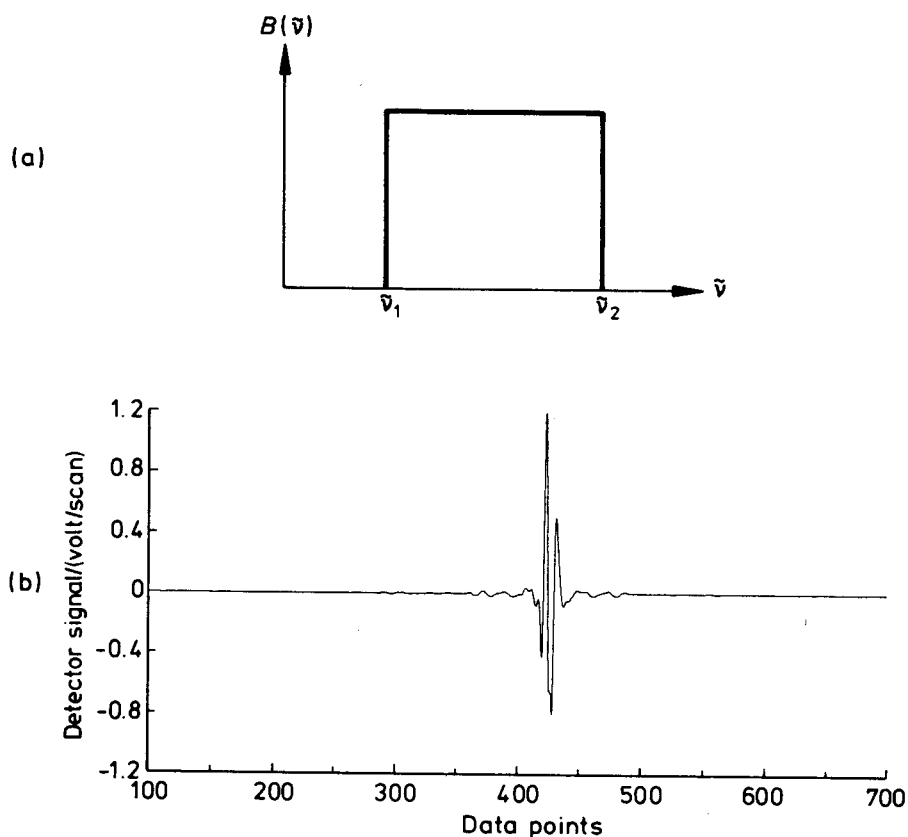


Figure 3.14 (a) Wavenumber domain spectrum of a broad band source and (b) the corresponding interferogram

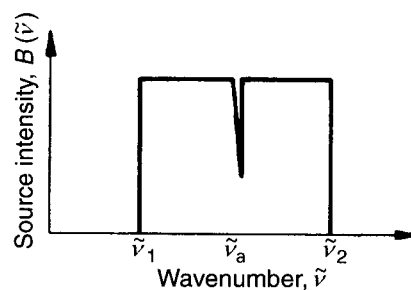


Figure 3.15 Wavenumber domain spectrum of a broad band source with a narrow absorption

If a single sharp absorption occurs at a wavenumber $\tilde{\nu}_a$, as shown in the wavenumber domain spectrum in Figure 3.15, the cosine wave corresponding to $\tilde{\nu}_a$ is not cancelled out and remains in the $I(\delta)$ versus δ plot, or interferogram, as it is often called. For a more complex set of absorptions the pattern of uncanceled cosine waves becomes more intense and irregular.

Figure 3.16(a) shows an interferogram resulting from the infrared absorption spectrum of air in the $400\text{--}3400\text{ cm}^{-1}$ region. The Fourier transformed spectrum in Figure 3.16(b)

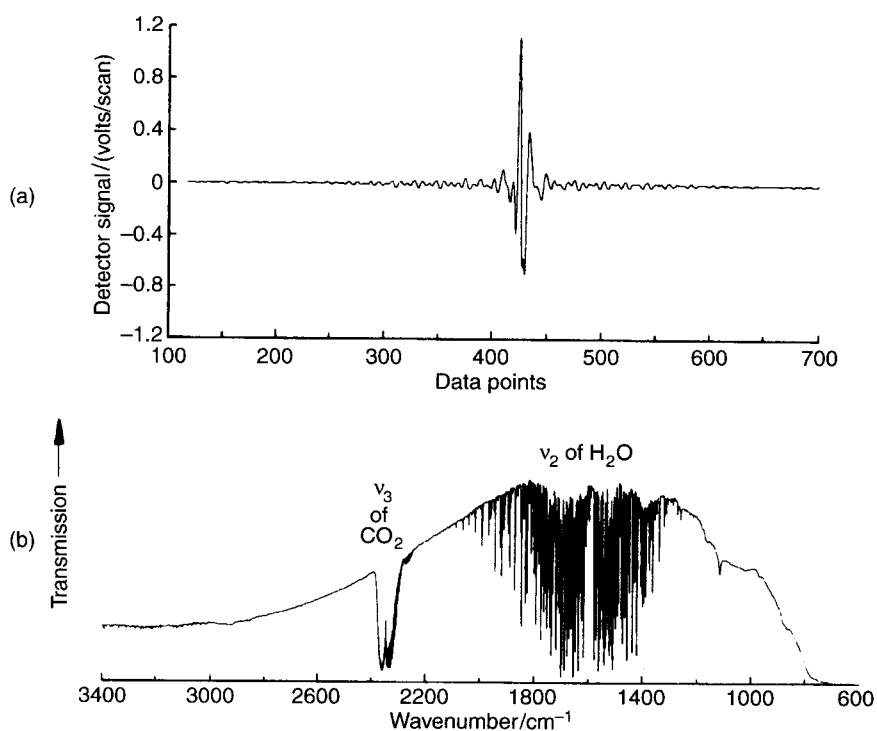


Figure 3.16 (a) Infrared interferogram of the absorption spectrum of air in the $400\text{--}3400\text{ cm}^{-1}$ region and (b) the Fourier transformed spectrum

shows strong absorption bands due to CO₂ and H₂O, that of H₂O showing much finer structure because it is a lighter molecule.

The interferogram is digitized before Fourier transformation by a dedicated computer. Figure 3.16(a) shows that, in this example, there are 600 data points in the part of the interferogram shown. The computer is limited in the number of data points it can handle and the user has a choice of having the data points closer together, and neglecting the outer regions of the interferogram, which gives a wider wavenumber range but lower resolution, or having the data points further apart, which gives higher resolution but a narrower wavenumber range. The resolution $\Delta\tilde{\nu}$ is always determined by how much of the interferogram can be observed which, in turn, depends on the maximum displacement δ of the mirror M₁. The resolution is given by

$$\Delta\tilde{\nu} = \frac{1}{\delta_{\max}} \quad (3.24)$$

One of the main design problems in an FTIR spectrometer is to obtain accurate, uniform translation of M₁ over distances δ_{\max} which may be as large as 1 m in a high-resolution interferometer.

As in all Fourier transform methods in spectroscopy, the FTIR spectrometer benefits greatly from the multiplex, or Fellgett, advantage of detecting a broad band of radiation (a wide wavenumber range) all the time. By comparison, a spectrometer that disperses the radiation with a prism or diffraction grating detects, at any instant, only that narrow band of radiation that the orientation of the prism or grating allows to fall on the detector, as in the type of infrared spectrometer described in Section 3.6.

In addition to the multiplex advantage, an FTIR spectrometer also has the advantage of a greater proportion of the source radiation passing through the instrument. The reason for this is that the narrow entrance slit (see Figure 3.2), which severely restricts the radiation throughput in a prism or grating spectrometer, is replaced by a circular aperture of larger area. This throughput advantage is known as the Jacquinot advantage.

3.4 Components of absorption experiments in various regions of the spectrum

Table 3.1 summarizes the details of typical sources, absorption cells, dispersing elements and detectors used in different regions of the electromagnetic spectrum.

3.4.1 Microwave and millimetre wave

In the microwave region tunable monochromatic radiation is produced by klystrons, each one being tunable over a relatively small frequency range, or a backward wave oscillator, tunable over a much larger range. Both are electronic devices. Absorption experiments are usually carried out in the gas phase, and mica windows, which transmit in this region, are placed on either end of the absorption cell, which may be several metres in length. Stark

Table 3.1 Elements of an absorption experiment in various regions of the spectrum

Region	Source	Absorption cell window	Dispersing element	Detector
Microwave	Klystron; backward wave oscillator	Mica	None	Crystal diode
Millimetre wave	Klystron (frequency multiplied); backward wave oscillator	Mica; polymer	None	Crystal diode; Golay cell; thermocouple; bolometer; pyroelectric
Far-infrared	Mercury arc	Polymer	Grating; interferometer	Golay cell; thermocouple bolometer; pyroelectric
Mid- and near-infrared	Nernst filament; globar	NaCl or KBr	Grating; interferometer	Golay cell; thermocouple; bolometer; pyroelectric; photoconductive semiconductor
Visible	Tungsten filament; xenon arc	Glass	Prism; grating; interferometer	Photomultiplier; photodiode; photographic plate
Near-ultraviolet	Deuterium discharge; xenon arc	Quartz	Prism; grating; interferometer	Photomultiplier; photodiode; photographic plate
Far-ultraviolet	Microwave discharge in noble gases; Lyman discharge	LiF (or no windows)	Grating	Photomultiplier; photodiode; photographic plate

modulation, in which an electric field is applied between a metal plate or septum, down the centre of the cell, and the cell walls, is often used to increase sensitivity. This also allows the measurement of the dipole moment of the absorbing molecule. Unusually, no dispersing element is needed as the source radiation is monochromatic. The detector is a crystal diode rectifier.

Millimetre wave radiation may also be generated by a klystron or backward wave oscillator but, since klystrons produce only microwave radiation, the frequency must be

multiplied, with consequent loss of power. Windows on the absorption cell are of the same material as used for the microwave or far-infrared regions, depending on the frequency range: this also applies to the detector. No dispersing element is required as the radiation is monochromatic.

Both microwave and millimetre wave radiation can be channelled in any direction by a waveguide made from metal tubing of rectangular cross-section, the dimensions depending on the frequency range. The absorption cell is also made from waveguide tubing.

3.4.2 Far-infrared

In the far-infrared region strong absorption by the water vapour normally present in air necessitates either continuously flushing the whole optical line with dry nitrogen or, preferably, evacuation.

Sources of radiation are all of lower than ideal intensity. One of the most commonly used is a mercury discharge in a quartz envelope, most of the higher-wavenumber radiation coming from the quartz rather than from the discharge plasma.

The windows of the absorption cell are made from polymer material such as polyethylene, poly(ethylene terephthalate; Terylene[®]) or polystyrene.

The dispersing element is commonly a Michelson type of interferometer (Section 3.3.3.2), with a beamsplitter made from a transmitting material, but a plane diffraction grating may also be employed. Various methods of employing a plane grating are used, but the Czerny–Turner system, shown in Figure 3.17, is one of the most common. The radiation from the source *S* passes through the absorption cell and enters at the slit *S*₁, which is separated by its focal length from the concave mirror *M*₁. This mirror is turned so as to reflect the radiation, now a parallel beam, onto the grating *G*, which disperses it and reflects it to *M*₂. This second mirror focuses the dispersed radiation onto the exit slit *S*₂ and thence to the detector *D*. The spectrum is scanned by smoothly rotating the grating.

A commonly used detector is a Golay cell, in which there is a far-infrared absorbing material, such as aluminium deposited on collodion, inside the entrance window of the cell.

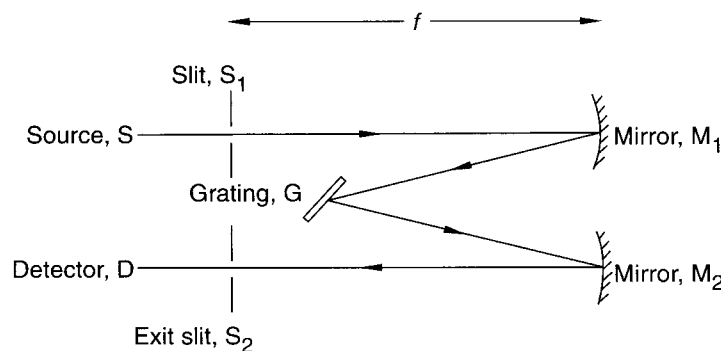


Figure 3.17 The Czerny–Turner grating mounting

The aluminium absorbs the radiation, heats up and transfers the heat to xenon gas contained in the cell. As the temperature of the gas varies the curvature of a flexible mirror of antimony-coated collodion, forming a part of the cell, changes. Reflection of a light beam from this mirror, which is on the outside of the Golay cell, indicates its curvature and therefore the intensity of radiation absorbed by the cell.

Thermocouples, bolometers and pyroelectric and semiconductor detectors are also used. The first three are basically resistance thermometers. A semiconductor detector counts photons falling on it by measuring the change in conductivity due to electrons being excited from the valence band into the conduction band.

3.4.3 *Near-infrared and mid-infrared*

Evacuation is not necessary in this region and sources are much less of a problem than they are in the far-infrared. A heated black body emits strongly in the near- and mid-infrared and a Nernst filament, consisting of a mixture of rare earth oxides, or a silicon carbide Globar, emulate a black body quite well.

Cell windows are usually made from sodium chloride, which transmits down to 700 cm^{-1} , or potassium bromide, down to 400 cm^{-1} . Concave mirrors, front-surface coated with aluminium, silver or gold, may be used to multiply reflect the radiation many times across the cell for higher absorbance by a gas-phase sample. If the sample is in solution the solvent must be carefully chosen. No single solvent is transparent throughout the region but, for example, carbon disulphide is transparent except for the region 1400 cm^{-1} to 1700 cm^{-1} , where tetrachloroethylene is transparent. A solid sample may be ground into a fine powder and, for wavenumbers less than 1300 cm^{-1} , made into a mull with Nujol[®] (a liquid paraffin) or, for observations over the whole range, ground together with potassium bromide and compressed under vacuum to give a KBr disk.

The dispersing element is usually a diffraction grating or an interferometer with a beamsplitter made from silicon-coated or germanium-coated quartz or calcium fluoride.

Detectors are similar in type to those for the far-infrared, namely thermocouples, bolometers, Golay cells or photoconductive semiconductors.

3.4.4 *Visible and near-ultraviolet*

Conventional, but not very intense, sources for these regions are a tungsten or tungsten-iodine filament lamp for the visible and a deuterium discharge lamp (more intense than a hydrogen discharge lamp), in a quartz envelope, for the near-ultraviolet. For both regions a much more intense source is a high-pressure xenon arc lamp in which an arc (usually direct current) is struck between two tungsten poles about 1 mm to 1 cm apart in xenon gas at about 20 atm pressure and contained in a quartz envelope. Such a lamp produces radiation down to about 200 nm.

Useful transparent materials for cell windows, lenses, and so on are Pyrex[®] glass for the visible and fused quartz for the visible and near-ultraviolet.

Dispersing elements may be either prisms (glass for the visible, quartz for the near-ultraviolet) or, more often, diffraction gratings for which a Czerny–Turner mounting, shown in Figure 3.17, may be used.

Detectors used are mostly photomultipliers, in which photons fall on a metal surface, such as caesium, which then emits electrons (photoelectrons; see Section 1.2). These electrons are subjected to an accelerating voltage and fall on a second surface, releasing secondary electrons, the process being repeated several times to give a large current amplification. Also used are photographic plates and arrays of photodiodes, both of which have the multiplex advantage of detecting a large range of wavelengths all the time.

A more recent, and superior, type of detector, which also benefits from the multiplex advantage, is the charge-coupled device (CCD). The CCD, as used for spectroscopy, has been developed from the CCD detector used in a camcorder.

A CCD is a two-dimensional array of silicon photosensors, each photosensor usually being referred to as a pixel. When radiation falls on a pixel, photoelectrons are produced in numbers proportional to the intensity of the radiation. A typical wavelength range to which the CCD is sensitive is 400–1050 nm, but this may be extended down to below 1.5 nm with a phosphor that converts short-wavelength into visible radiation.

Whereas a photodiode array is typically a linear array consisting of a single row of photodiodes, the CCD is a two-dimensional array, consisting of rows and columns of pixels. In this sense it resembles a photographic plate. Each row of the CCD should, ideally, give the same spectrum (wavelength versus intensity). Computer addition of the signals from pixels in the same column then produces a spectrum with a much higher signal-to-noise ratio than would result from a one-dimensional array. A typical CCD may contain about 2000 columns and 800 rows of pixels, the area of each pixel being about $15\ \mu\text{m} \times 15\ \mu\text{m}$.

3.4.5 *Vacuum- or far-ultraviolet*

As for the far-infrared, absorption by air in the vacuum-ultraviolet (VUV) necessitates evacuation of the optical path from source to detector. In this region it is oxygen which absorbs, being opaque below 185 nm.

Sources of VUV radiation cause something of a problem. A deuterium discharge lamp emits down to 160 nm, a high-voltage spark discharge in helium produces radiation from 100 nm to 60 nm, and microwave-induced discharges in argon, krypton or xenon cover the range 200 nm to 105 nm. A much larger continuum range, from the visible down to about 30 nm, is provided by a Lyman source in which a large condenser is repetitively discharged through a low-pressure gas contained in a glass capillary. The most ideal source of VUV radiation is the synchrotron radiation source, which will be discussed in Section 8.1.1.

Lithium fluoride is transparent down to about 105 nm, below which windowless systems must be used with differential pumping.

The dispersing element is a diffraction grating preferably used under conditions of grazing incidence (θ in Equation 3.9 about 89°) to improve the reflectance. The grating may also be concave to avoid the use of a focusing mirror.

Photomultipliers or photographic plates may be employed as detectors.

3.5 Other experimental techniques

3.5.1 *Attenuated total reflectance spectroscopy and reflection-absorption infrared spectroscopy*

The attenuated total reflectance (ATR) technique is used commonly in the near-infrared for obtaining absorption spectra of thin films and opaque materials. The sample, of refractive index n_1 , is placed in direct contact with a material which is transparent in the region of interest, such as thallium bromide/thallium iodide (known as KRS-5), silver chloride or germanium, of relatively high refractive index n_2 , so that $n_2 \gg n_1$. Then, as Figure 3.18 shows, radiation falling on the interface may be totally reflected, provided the angle i is greater than a certain critical value. However, the radiation penetrates the sample to a depth of about 20 μm and may be absorbed by it. As a wavelength at which absorption takes place is approached, the refractive index n_1 , which is wavelength-dependent, changes rapidly, and the greater is this change the greater is the degree of attenuation of the radiation. Therefore the intensity of the reflected light varies with wavelength in a way resembling an absorption spectrum. In practice, multiple internal reflections are used to enhance the attenuation.

Whereas ATR spectroscopy is most commonly applied in obtaining infrared absorption spectra of opaque materials, reflection-absorption infrared spectroscopy (RAIRS) is usually used to obtain the absorption spectrum of a thin layer of material adsorbed on an opaque metal surface. An example would be carbon monoxide adsorbed on copper. The metal surface may be either in the form of a film or, of great importance in the study of catalysts, one of the particular crystal faces of the metal.

The radiation from an infrared source is directed at a very small (grazing) angle of incidence onto the surface. The reflected and then dispersed light gives the absorption spectrum of the adsorbed material. Interpretation of the spectrum provides information on the way in which the material is adsorbed. For example, it is possible to distinguish carbon monoxide molecules lying perpendicular to the metal surface from those lying parallel to it. This orientation of the adsorbate may change with the degree of surface coverage.

3.5.2 *Atomic absorption spectroscopy*

Atomic absorption spectroscopy (AAS) is complementary to atomic emission spectroscopy (see Section 3.5.3) and became available for a wide range of atoms in the mid-1950s.

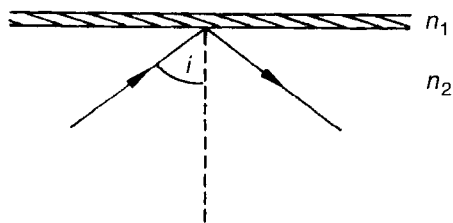


Figure 3.18 Total reflection of radiation in a medium of refractive index n_2 by a thin film of refractive index n_1 , where $n_2 \gg n_1$

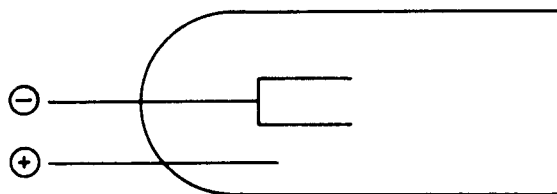


Figure 3.19 A hollow cathode lamp

The main problem in this technique is getting the atoms into the vapour phase, bearing in mind the typically low volatility of many materials to be analysed. The method used is to spray, in a very fine mist, a liquid molecular sample containing the atom concerned into a high-temperature flame. Air mixed with coal gas, propane or acetylene, or nitrous oxide mixed with acetylene, produce flames in the temperature range 2100 K to 3200 K, the higher temperature being necessary for such refractory elements as Al, Si, V, Ti and Be.

The source radiation which passes through the flame is not a continuum, as would normally be used in absorption spectroscopy, but a hollow cathode lamp. The lamp, shown in Figure 3.19, contains a tungsten anode, a cup-shaped cathode made from the element to be analysed, and a carrier gas, such as neon, at about 5 Torr. When a voltage is applied a coloured discharge appears and the positive column, in which mainly neutral atom emission occurs, is confined to the inside of the cathode by choice of voltage and carrier gas pressure. The radiation emitted, apart from that from the carrier gas, is from the atom to be observed in absorption. Figure 3.20 shows just two atomic emission lines λ_1 and λ_2 from the hollow cathode. If, for example, λ_1 represents a transition from an excited state to the *ground* state of the atom then, as shown, this can be absorbed by the flame. However, if λ_2 represents a transition between two excited states, it cannot be absorbed since, even at a flame temperature of 3000 K, there is almost no population of any excited states because the separations ΔE from the ground state are so large (see Equation 2.11). The dispersing

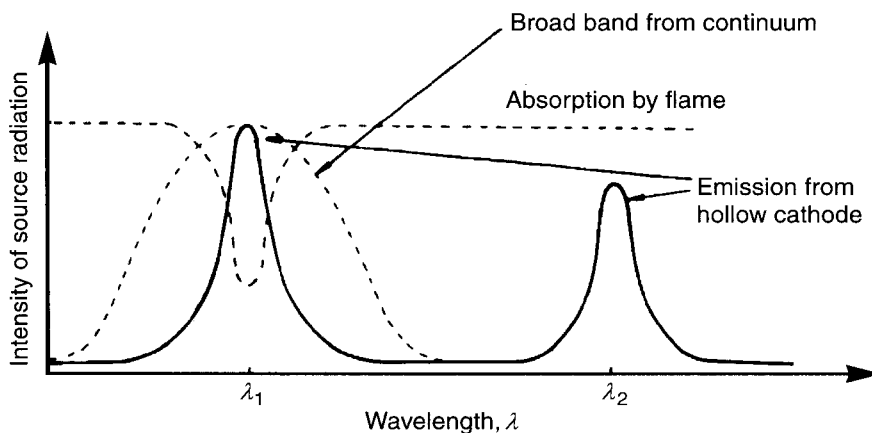


Figure 3.20 The principle of atomic absorption spectroscopy

element of the spectrometer is set so that the photoelectric detector receives radiation of wavelength λ_1 only. Calibration is achieved by spraying a mist of a solution, containing a known concentration of the atom concerned, into the flame.

The advantage of using a hollow cathode rather than a broad-band continuum is illustrated in Figure 3.20. By using a continuum, sensitivity would be lost because only a relatively small amount of radiation would be absorbed.

3.5.3 Inductively coupled plasma atomic emission spectroscopy

Emission spectroscopy is a very useful analytical technique in determining the elemental composition of a sample. The emission may be produced in an electrical arc or spark but, since the mid-1960s, an inductively coupled plasma has increasingly been used.

For inductively coupled plasma atomic emission spectroscopy (ICP-AES) the sample is normally in solution but may be a fine particulate solid or even a gas. If it is a solution, this is nebulized, resulting in a fine spray or aerosol, in flowing argon gas. The aerosol is introduced into a plasma torch, illustrated in Figure 3.21.

The torch consists of three concentric quartz tubes. The argon aerosol passes up the central tube. There is an auxiliary supply of argon in the outer tube to provide cooling and, between these, there is a further supply of flowing argon. Radiofrequency radiation, with a frequency of 25–60 MHz and a power of 0.5–2.0 kW, is supplied through a copper coil around the outer tube. A high-voltage spark is applied to initiate the plasma flame, which is then maintained through the inductive heating of the gas by the radiofrequency radiation. The flow of argon in the central tube can be varied to adjust the height of the flame.

The temperature of the plasma in the region of observation is typically 7000–8000 K, and all molecules contained in the aerosol sample are atomized. The majority of the atoms are also

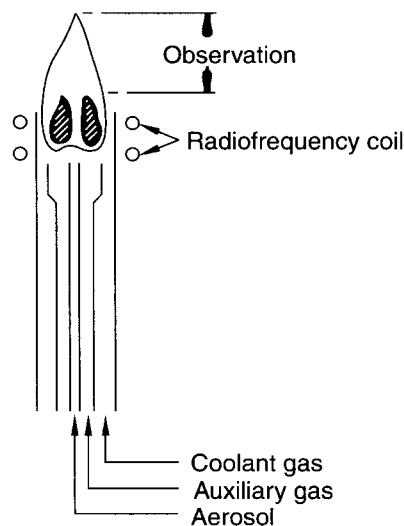


Figure 3.21 A plasma torch for inductively coupled plasma atomic emission spectroscopy

singly ionized and many of the ions are produced in various excited electronic states. The radiation emitted from these excited ions is then analysed by a spectrometer, which usually operates in the 800–190 nm region, evacuation being necessary if wavelengths lower than 190 nm are important. The wavelengths are dispersed and resolved by a diffraction grating.

There are two general types of spectrometer. In a scanning spectrometer there is a fixed photomultiplier detector and the grating is rotated smoothly so that a single detector covers the complete range of wavelengths in which the emission spectrum occurs. In a polychromator, in contrast, the grating is fixed and a number of detectors are arranged at positions corresponding to the emission wavelengths of the atoms or ions being determined. In this way, simultaneous, multielement analysis can be achieved.

A wider range of elements is covered by ICT–AES than by atomic absorption spectroscopy. All elements, except argon, can be determined with an inductively coupled plasma, but there are some difficulties associated with He, Ne, Kr, Xe, F, Cl, Br, O and N.

The detection limits of $1\text{--}100\ \mu\text{g dm}^{-3}$ are similar for both techniques.

3.5.4 Flash photolysis

Transient species, existing for periods of time of the order of a microsecond (10^{-6} s) or a nanosecond (10^{-9} s), may be produced by photolysis using far-ultraviolet radiation. Electronic spectroscopy is one of the most sensitive methods for detecting such species, whether they are produced in the solid, liquid or gas phase, but a special technique, that of flash photolysis devised by Norrish and Porter in 1949, is necessary.

Figure 3.22 illustrates the general principles applied to a gas-phase absorption experiment. The flashlamps F contain electrodes inside quartz envelopes containing a noble gas. High-capacity condensers are discharged between the electrodes, and visible and ultraviolet radiation passes from F through the walls of the quartz cell C. The parent molecule in C is photolysed, for example $\text{NH}_3 \rightarrow \text{NH}_2 + \text{H}$, by the far-ultraviolet radiation produced in the flash. In order to observe the absorption spectrum of, say, NH_2 at its optimum concentration, a pulse of a continuum source S is initiated which passes through the cell to the spectrograph (photographic recording) or spectrometer (photoelectric recording), which records the spectrum. The process of photolysis flash followed by source flash may be repeated many times in order to accumulate the spectrum, and a liquid or gaseous sample may be flowed through the cell. An important variable parameter is the delay time between the photolysis

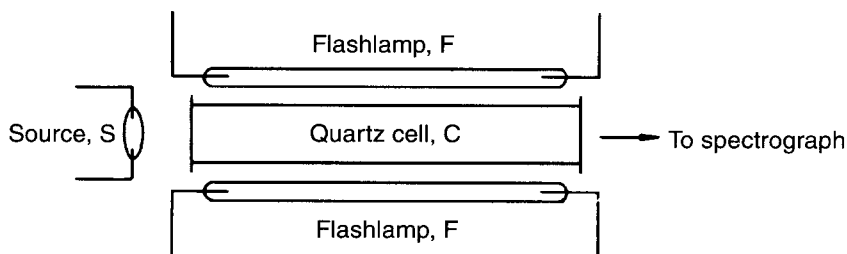


Figure 3.22 Principal components of an early flash photolysis absorption experiment

and source flashes and is typically in the region 1 μs to 1000 μs , depending on the species and the conditions in the cell.

Pulsed lasers (Chapter 9) may be used both for photolysis and as a source. Since the pulses can be extremely short, of the order of a few picoseconds or less, species with comparably short lifetimes, such as an atom or molecule in a short-lived excited electronic state, may be investigated.

3.6 Typical recording spectrophotometers for the near-infrared, mid-infrared, visible and near-ultraviolet regions

Perhaps the most common type of spectrometer that we encounter in the laboratory is the double-beam spectrophotometer for use in the mid-infrared, near-infrared, visible or near-ultraviolet region. 'Double beam' refers to the facility of having two beams of continuum radiation, one for a sample cell containing, say, a solution of A in a solvent B and the other for a reference cell containing only B. The absorption spectrum recorded with cells of identical pathlengths in each beam is that of solution-minus-solvent, in this case that of A alone. It is important to realize, however, that if the solvent is absorbing nearly all of the radiation at a particular wavelength the value of the absorbance for solution-minus-solvent cannot be meaningful.

Figure 3.23 illustrates the layout of a typical mid-infrared and near-infrared spectrophotometer. The source radiation is split into the reference and sample beams by two toroidal mirrors (concave but with different curvature in two perpendicular directions – like a section of the side of a barrel). Eventually they strike the rotating sector mirror which has alternate regions which either transmit the sample beam or reflect the reference beam towards the next toroidal mirror. This receives, alternately, light from the reference and sample beams which are reflected to the diffraction grating by a parabolic mirror. Such a mirror makes parallel all radiation emanating from the focus of the parabola whichever part of the mirror it strikes. The width of the entrance and exit slits may determine the resolution when they are relatively wide, but when they are narrowed it is, eventually, the number of grooves on the grating that limits the resolution (Equations 3.3 and 3.8). The detector receives radiation alternately from the sample and reference beams, and phase-sensitive treatment of the signal allows these two to be separated.

In the method of recording in Figure 3.23 the absorbance in the sample beam relative to that in the reference beam is obtained by inserting an optical attenuator into the reference beam which is attenuated until the two detected signals are equal. This optical null method has the disadvantage of reducing drastically the intensity in the reference beam when the sample is absorbing strongly. In the infrared this method has been largely replaced by ratio recording in which the intensity in the reference beam, I_0 , and that in the sample beam, I , are ratioed by a microprocessor to give the absorbance A of the sample relative to that of the reference by Equation (2.16). This method is particularly advantageous when absorbance is high (i.e. when the transmittance is low).

Figure 3.24 illustrates a typical optical layout for a visible and near-ultraviolet double-beam recording spectrophotometer. The arrangement is very similar to that in Figure 3.23

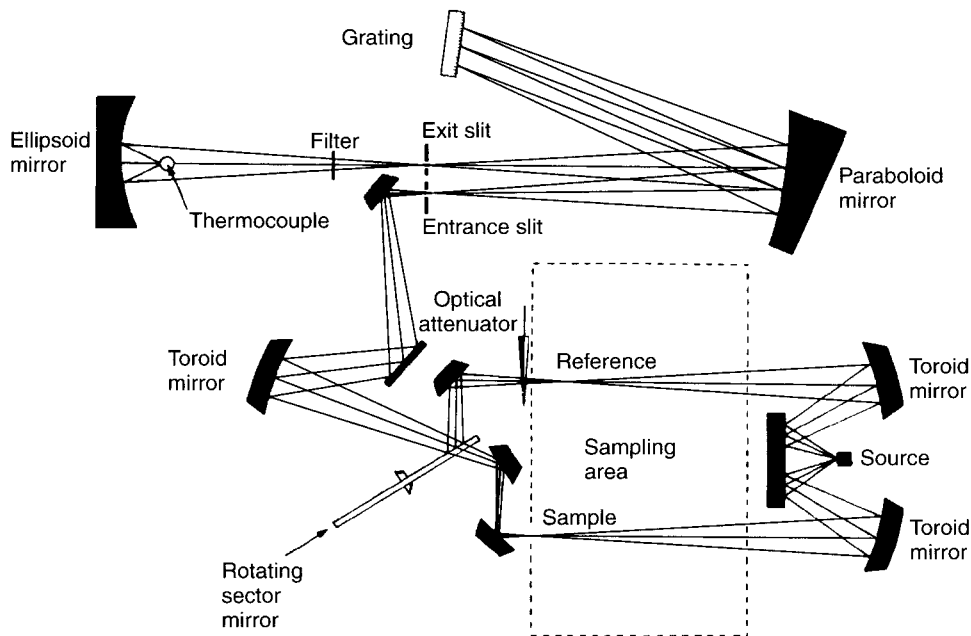


Figure 3.23 A typical double-beam recording mid-infrared and near-infrared spectrophotometer

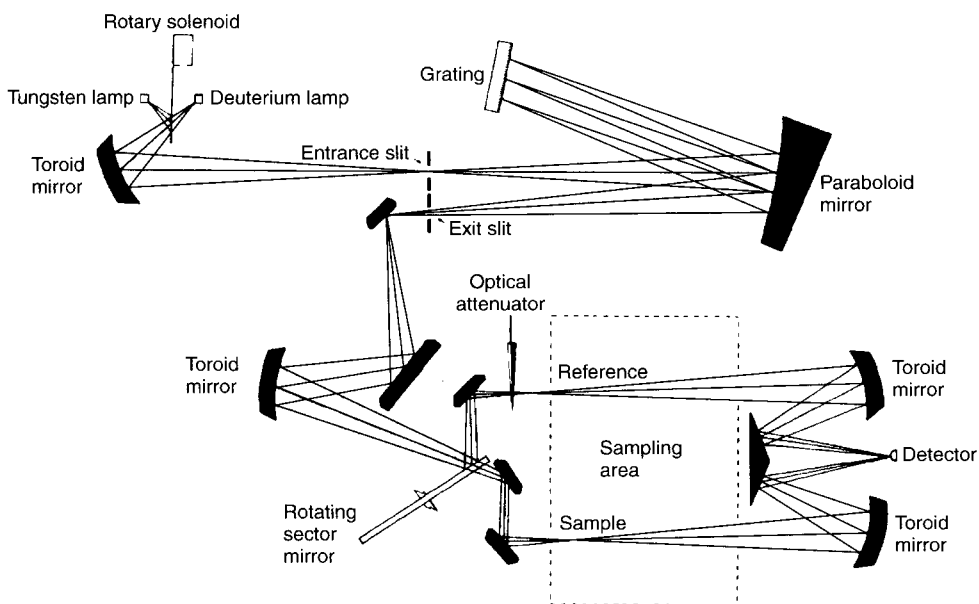


Figure 3.24 A typical double-beam recording visible and near-ultraviolet spectrophotometer

for an infrared instrument except that the optical line is reversed in that the positions of source and detector are interchanged. A mirror is rotated in order to change from the tungsten to the deuterium lamp for near-ultraviolet operation.

Typical regions covered by these instruments are 200 cm^{-1} to 5000 cm^{-1} ($50\text{ }\mu\text{m}$ to $2\text{ }\mu\text{m}$) in the infrared, and $11\,100\text{ cm}^{-1}$ to $51\,300\text{ cm}^{-1}$ (900 nm to 195 nm) in the visible and near-ultraviolet. This leaves a gap from $0.9\text{ }\mu\text{m}$ to $2\text{ }\mu\text{m}$, which is filled by some spectrophotometers.

Exercise

3.1 At $18\text{ }^{\circ}\text{C}$ the refractive index of fused quartz varies with wavelength as follows:

λ/nm	n	λ/nm	n
185.47	1.5744	274.87	1.4962
193.58	1.5600	303.41	1.4859
202.55	1.5473	340.37	1.4787
214.44	1.5339	396.85	1.4706
226.50	1.5231	404.66	1.4697
250.33	1.5075	434.05	1.4670

Plot λ against n and hence obtain the resolving power of a fused quartz prism, with a base length of 3.40 cm , at 200 nm , 250 nm , 300 nm and 350 nm . What is the resolution, in nanometres, at these wavelengths? How would the resolving power and resolution be affected, quantitatively, by using two such prisms in tandem?

Bibliography

- Bousquet, P. (1971) *Spectroscopy and its Instrumentation*, Adam Hilger, London.
 Dean, R. (1997) *Atomic Absorption and Plasma Spectroscopy, 2nd edition*, John Wiley, Chichester.
 Griffiths, P. R. and De Haseth, J. A. (1986) *Fourier Transform Infrared Spectrometry*, John Wiley, Chichester.
 Harihan, P. (1991) *Basics of Interferometry*, Academic Press, San Diego, CA.
 Harrison, G. R., Lord, R. C. and Loofbourow, J. R. (1948) *Practical Spectroscopy*, Prentice-Hall, Englewood, NJ.

- Hecht, H. and Zajac, A. (1974) *Optics*, Addison-Wesley, Reading, MA.
- Jenkins, F. A. and White, H. E. (1957) *Fundamentals of Optics*, McGraw-Hill, New York.
- Longhurst, R. S. (1957) *Geometrical and Physical Optics*, Longman, London.
- Sawyer, R. A. (1963) *Experimental Spectroscopy*, Dover, New York.
- Sneddon, J., Thiem, T. and Lee, Y.-I. (1997) *Lasers in Atomic Spectroscopy*, John Wiley, New York.

